Journal of Soft Computing in Civil Engineering 6-4 (2022) 130-152

Contents lists available at SCCE

Journal of Soft Computing in Civil Engineering

Journal homepage: www.jsoftcivil.com

Application of Machine Learning Technique in Predicting the Bearing Capacity of Rectangular Footing on Layered Sand under Inclined Loading

Vishal Panwar, Rakesh Kumar Dutta*

Department of Civil Engineering, NIT Hamirpur, Himachal Pradesh, India
Corresponding author: *vipsarahan17@gmail.com*

https://doi.org/10.22115/SCCE.2022.343236.1445

ARTICLE INFO

Article history:
Received: 20 May 2022
Revised: 20 May 2022
Accepted: 01 October 2022

Keywords:
Bearing capacity;
Layered sand;
Rectangular footing;
Inclined load;
Machine learning technique.

ABSTRACT

The aim of the present study is to apply machine learning technique to predict the ultimate bearing capacity of the rectangular footing on layered sand under inclined loading. For this purpose, a total 5400 data based on the finite element method for the rectangular footing on layered sand under inclined loading were collected from the literature to develop the machine learning model. The input variables chosen were the thickness ratio (0.00 to 2.00) of the upper dense sand layer, embedment ratio (0 to 2), the friction angle of upper dense (410 to 460) sand and lower loose (310 to 360) sand layer and inclination (00 to 450) of the applied load with respect to vertical. The output is the ultimate bearing capacity. Further, the impact of the individual variable on the bearing capacity was also assessed by conducting sensitivity analysis. The results reveal that, the load inclination is the major variable affecting the bearing capacity at embedment ratio 0, 1 and 2. Finally, the performance of the developed machine learning model was assessed using six assessing statistical parameters. The results reveal that the developed model was performing satisfactorily for the prediction of the ultimate bearing capacity of the rectangular footing on layered sand under inclined loading.

How to cite this article: Panwar V, Dutta RK. Application of machine learning technique in predicting the bearing capacity of rectangular footing on layered sand under inclined loading. J Soft Comput Civ Eng 2022;6(4):130–152. https://doi.org/10.22115/scce.2022.343236.1445

1. Introduction

The footing transfers the load of the superstructure to the soil beneath it. The depth-to-width ratio determines whether a footing is shallow or deep. The load must be conveyed beneath the footing without causing it to settle or shear. Experimental, numerical, and analytical investigations using vertical [1–9] and inclined [10–13] loading have been used to determine the ultimate bearing capacity of strip, circular, square, and rectangular footings on single layer or layered soils. In [7], a comparison was made between the various experimental methods, limit equilibrium approaches, and finite element studies for determining the bearing capacity of the strip footing on layered soils under vertical loading. The authors concluded that the ratio of the thickness of the first layer to the thickness of the base was the deciding element and had a greater impact than the other variables considered. There is no ultimate bearing capacity equation for the rectangular footing on layered sand under inclined loading as evident from literature [10–13]. In such cases, the only way to determine the bearing capacity is to conduct expensive and time-consuming experimental or numerical research. Another method is to calibrate and fit the experimental or numerical data to create a mathematical model to explain the interactions among the numerous variables. Because of their ability to store, learn, and represent the dynamic interaction between numerous variables without any prior ideas regarding bearing capacity, machine learning approaches are a superior alternative for modelling. Further, the problem of predicting the bearing capacity of shallow footings under inclined loading is very complex especially in the layered granular soils and not yet entirely understood. This fact has encouraged researchers [14–28] to apply the machine learning technique to bearing capacity and settlement prediction under vertical and eccentric loading. In [22], in addition to limit equilibrium and numerical methods for calculating the ultimate bearing capacity of strip footings supported by multilayered soils under vertical loading, machine learning technique has also been successfully applied and used. The prediction of bearing capacity of strip footing resting on layered soil under vertical loading using various machine learning approaches (generalized reduced gradient, genetic programming, artificial neural network, and evolutionary polynomial regression) was reported. The study concluded that artificial neural network outperformed other techniques (generalized reduced gradient, genetic programming, and evolutionary polynomial regression). The ultimate bearing capacity of strip footing on multilayered soil under vertical loading was predicted by [23] using artificial neural network and certain metaheuristic approaches such as dragonfly approach, Harris hawk's optimization, and sparse polynomial chaos expansions. Using elephant herding optimization, shuffling frog leaping algorithm, salp swarm algorithm, wind-driven optimization, and artificial neural network to produce neural ensembles, The researcher [17] evaluated the usefulness of merging a black hole algorithm and a multi-verse optimizer with an artificial neural network (ANN) to produce hybrid models, the black hole algorithm and multi-verse optimizer (MVO) can improve the artificial neural network's accuracy. The author also indicated that MVO-ANN can be employed as a trustworthy method for the realistic estimation of bearing capacity. Artificial neural networks to simulate 2430 finite element models to evaluate the bearing capacity in shallow footings and to optimize the performance of the model using an imperialist competitive strategy was employed by [18]. The shear strength using salp swarm algorithm was predicted by [19] and the authors concluded that it could serve as a viable

alternative to standard approaches. To forecast the factor of safety against slope failures, multi-layer perceptron (MLP), Gaussian process regression, multiple linear regression, simple linear regression, and support vector regression was used by [20]. The authors concluded that the MLP performed better than other machine learning-based models. According to the literature, the novelty of this work resides in the fact that no work has yet been published that uses machine learning to predict the bearing capacity of rectangular footings constructed on layered sand under inclined loading. This paper proposes the use of machine learning to predict the bearing capacity of a rectangular footing constructed on layered sand and loaded at an angle. In addition, most existing investigations on rectangular footings on layered sand under vertical and inclined loading employed experimental or numerical approaches. Experimentally or numerically, the influence of embedment ratio on the bearing capacity of the rectangular footing on layered sand under inclined has not been studied. The following objectives were taken into consideration when developing this model.

i. To determine the parameters that influence the bearing capacity of the rectangular footing on layered sand under inclined load, as well as to examine the relationships that exist between those parameters.
ii. To design a machine learning model for predicting bearing capacity and to test the model's accuracy using statistical parameters.
iii. To perform sensitivity analysis to examine the impact of various parameters on output bearing capacity.
iv. To create an empirical model utilizing a machine learning approach to make a prediction about the bearing capacity of a rectangular foundation placed on layered sand and subjected to inclined loading.

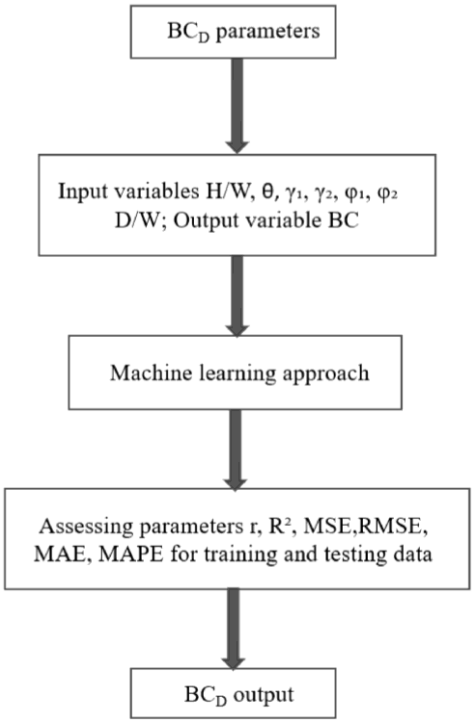

Fig. 1. Simplified illustration of machine learning approach.

The footing embedment ratio (D/W), upper dense sand layer thickness ratio (H/W), unit weight and friction angle of the upper dense (γ_1, φ_1) and lower loose (γ_2, φ_2) sand layers and load inclination (θ) with respect to vertical were all employed as input variables. The schematic of the machine learning approach is depicted in Figure 1.

2. Machine learning technique

The application of artificial neural network (ANN) attempts to mimic the neural system and the functions of the human brain. Without any prior expectations, ANN modelling may differentiate intricate nonlinear linkages between the input and output variables. Furthermore, unlike conservative techniques, ANN can use raw data (input) without any editing or pre-processing, making it more helpful and less expensive. Before making any interpretation of new information, an ANN must be trained, for which several algorithms were available in the literature. A feed forward back propagation technique is the most adaptable and effective for multilayer neural networks [16,29,30]. Interconnected layers make up the backpropagation (BP) algorithm (input, hidden and output). The output of the input layer's neuron or node was supplied as an input to a hidden layer node, and the hidden layer's neuron or node's output was finally transferred to the output layer. The number of hidden layers and the number of hidden layers is determined by the problem at hand. As a result, researchers had to resort to a time-consuming trial-and-error method. In the BP network, all nodes (excluding the input layer) had an activation function and a bias node. A constant input is included in the bias. The aggregated output is filtered by the activation function. In ANN, activation functions were utilised depending on the objective. The output layer created computed vectors of the output corresponding to the problem's solution. The input/output data were often expressed as vectors (named as training pairs). The method is repeated for the training pairs in the data until the network error is aggregated to a brink, which is determined using an error function (RMSE, root mean square error). For connecting the hidden and output layers, the same approach was used. The above technique was also performed during the network's training (input to the hidden and hidden to the output layer). Iteration refers to a single step in the overall training sequence. As a result, the number of iterations is increased until the needed output is achieved (error is within the specified limit). ANN has the advantage of being a more reliable and precise alternative to regression-based methods and formulas. This is because this modelling strategy lacks a formal expression between input and output variables. ANN has the disadvantage of requiring a lengthy trial-and-error procedure to identify network properties such as hidden layers and neurons.

3. Data

A total of 5400 data points were collected using the ABAQUS software and the C3D8R element to determine the bearing capacity of a rectangular footing on layered sand (dense sand over loose sand) under inclined loading. Importantly, none of these 5400 data had previously been reported in a machine learning study. The modelling utilised the data generated by the numerical study described in [5,13]. Table 1 provides additional information about the parameters used. Using the

parameters shown in Table 1 for various embedment ratios, additional numerical research was conducted.

Table 1
Details of parameters varied for modelling.

Property	Range of variation											
Friction angle (Deg.)	31°	32°	33°	34°	35°	36°	41°	42°	43°	44°	45°	46°
Unit weight(kN/m^3)	14.5	15.0	15.5	16.0	16.5	17.0	19.5	20.0	20.5	21.0	21.5	22.0
Modulus (MPa)	22.8	26.4	31.2	33.6	38.4	43.2	68.4	74.4	82.8	91.2	102.0	120.0
Dilation angle (Deg.)	1°	2°	3°	4°	5°	6°	11°	12°	13°	14°	15°	16°
Poission ratio	0.35	0.34	0.33	0.32	0.31	0.30	0.30	0.28	0.26	0.24	0.22	0.20
Embedment ratio	0, 1 and 2											
Thickness ratio	0.0, 0.50, 1.00, 1.50, 2.00											
Load inclination (Deg.)	0˚, 5˚, 10˚, 15˚, 20˚, 25˚, 30˚, 35˚, 40˚, 45˚											

Table 2
Range of data used for the training and testing at different embedment ratio.

Input & output parameters	Training data set				Testing data set			
	Minimum	Maximum	Mean	Standard deviation	Minimum	Maximum	Mean	Standard deviation
D/W	0	0	0	0	0	0	0	0
H/W	0	2	0.929	0.69	0	2	1.16	0.70
γ_1	19.5	22	20.75	0.85	19.5	22	20.75	0.85
γ_2	14.5	17	15.85	0.85	14.5	17	15.51	0.81
φ_1	41	46	43.5	1.70	41	46	43.50	1.70
φ_2	31	36	33.70	1.70	31	36	33.02	1.62
θ	0	45	22.5	14.36	0	45	22.50	14.37
BC_{DA}	75.41	6212.64	926.87	931.29	72.526	6524.59	1080.91	1176.79
D/W	1	1	1	0	1	1	1	0
H/W	0	2	0.92	0.69	0	2	1.171	0.70
γ_1	19.5	22	20.75	0.85	19.5	22	20.75	0.85
γ_2	14.5	17	15.87	0.84	14.5	17	15.50	0.81
φ_1	41	46	43.5	1.70	0	45	22.50	14.37
φ_2	31	36	33.71	1.69	41	46	43.50	1.70
θ	0	45	22.5	14.36	31	36	33	1.63
BC_{DA}	371.62	13973.31	3061.58	2179.27	358.62	16021.20	3564.47	2804.63
D/W	2	2	2	0	2	2	2	0
H/W	0	2	0.92	0.69	0	2	1.16	0.70
γ_1	19.5	22	20.75	0.85	19.5	22	20.75	0.85
γ_2	14.5	17	15.85	0.84	14.5	17	15.50	0.81
φ_1	41	46	43.5	1.70	41	46	43.5	1.70
φ_2	31	36	33.71	1.69	31	36	33.00	1.63
θ	0	45	22.50	14.36	0	45	22.50	14.37
BC_{DA}	1398.63	19826.43	4883.45	2862.87	1348.63	25733.37	5616.06	4002.85

As a result, for the model creation in this study, seven input (D/W, H/W, γ_1, γ_2, φ_1, φ_2, θ) and one output (BC_{DP}) variables were included. Table 2 shows the lowest, maximum, average, and standard deviation of all gathered data for training and testing at varied embedment ratios. It should be mentioned that the data is separated into 70 % and 30 % for training and testing purposes at each embedment ratio. The thickness ratio (H/W), load inclination angle (θ), unit weight of higher dense (γ_1) and lower loose sand layer (γ_2), Friction angle of upper dense (φ_1)

and lower loose sand (φ_2) layer, and embedment ratio (D/W) all affect the rectangular footing's bearing capacity (BC_D). As a result, a model was created with all the variables as inputs, and the output was the bearing capacity (BC_D), which is defined as follows in equation (1).

$$BC_D = [q_u]_{\langle H/W,\theta,\varphi_1,\varphi_{2,}\gamma_1,\gamma_{2,}D/W\rangle} \quad (1)$$

$[q_u]_{\langle H/W,\theta,\varphi_1,\varphi_{2,}\gamma_1,\gamma_{2,}D/W\rangle}$ = Bearing capacity of rectangular footing on layer sand under inclined loading

A model was created based on the input and output. The proposed model was evaluated using a model that assessed metrics such as correlation (coefficient (r), coefficient of determination (R2), mean square error (MSE), root mean square error (RMSE), mean absolute error (MAE), and mean absolute percentage error (MAPE).

4. Model development

Modeling was done with the WEKA software. It is pertinent to mention here that during K-fold cross-validation, WEKA software randomly divides the original sample into K subsamples. One subsample is used for model validation, while the remaining K-1 subsamples are used for model training. The procedure is then repeated K times, with each of the K subsamples serving as validation data exactly once. The K results from the folds can then be averaged to produce a single estimate. The value of K used in the applied K-fold- CV technique by WEKA is 10 in the present analysis for the model development. The initial step in the model construction process is to train using the training data. The connection weights were generated after the network had been trained. According to [31], the number of hidden layers was initially set to one, with the number of hidden layer neurons accounting for two-thirds of the input variable for each embedment ratio. For the creation of the model in this study, a default-learning rate of 0.7 was chosen. The next step is to determine the number of iterations that are compatible with mean square error (MSE) and coefficient of determination (R^2), with MSE being the smallest and R^2 being as near to 1 as possible. The number of hidden layer neurons also had a substantial impact on the mean square error (MSE) and coefficient of determination (R^2). Figure 2 demonstrates how the MSE changes as the number of iterations increases for each embedment ratio (0, 1 and 2). The MSE reduces as the number of iterations grows and remains nearly constant or increases after reaching the minimal value, according to this graph. The smallest value of MSE was recorded at 1360, 960, and 840 number of iterations at varied embedment ratios, as shown in Figure 2. The next stage was to determine the best number of hidden layer neurons to use for model construction.

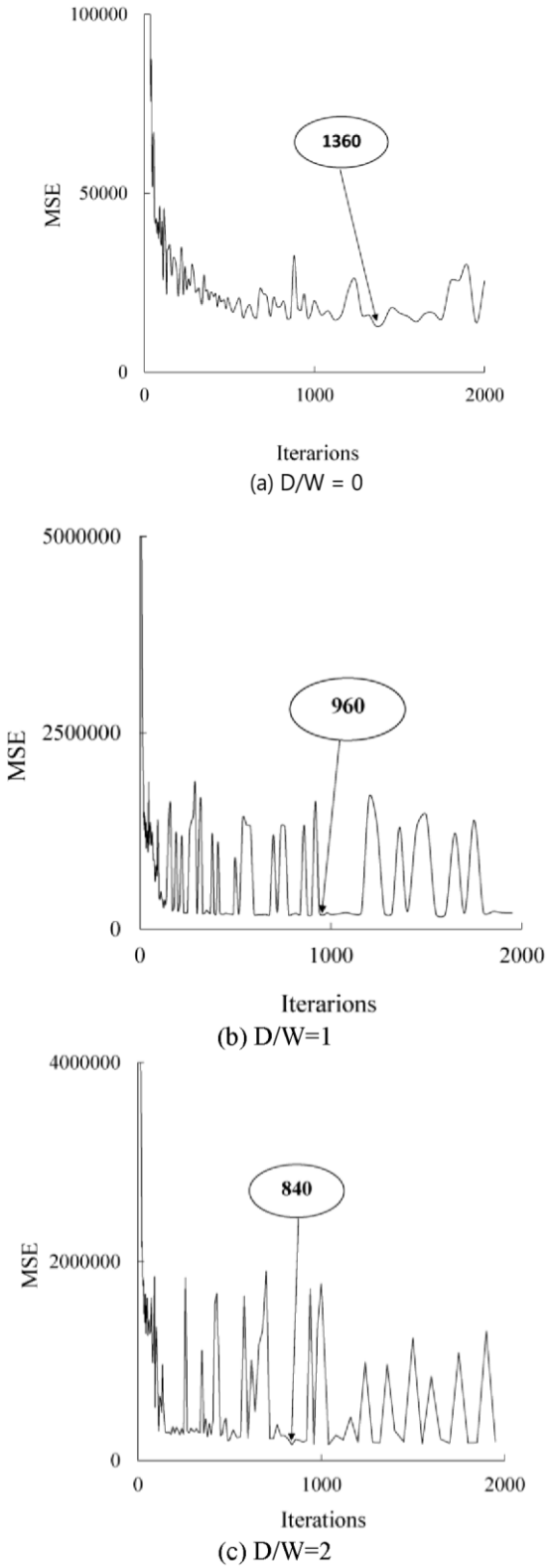

Fig. 2. Estimation of the optimum number of iterations at different embedment ratio.

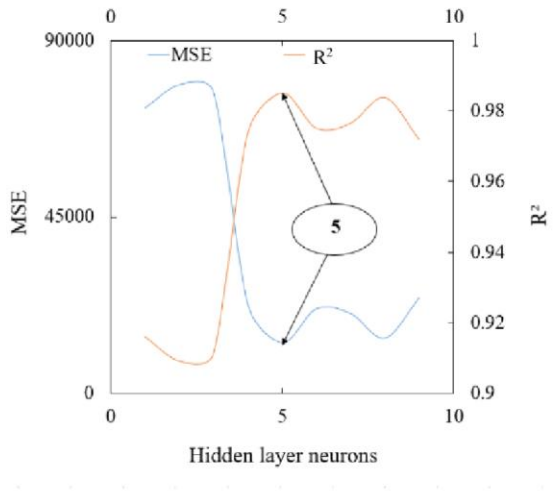

(a) D/W=0

(a) D/W=0

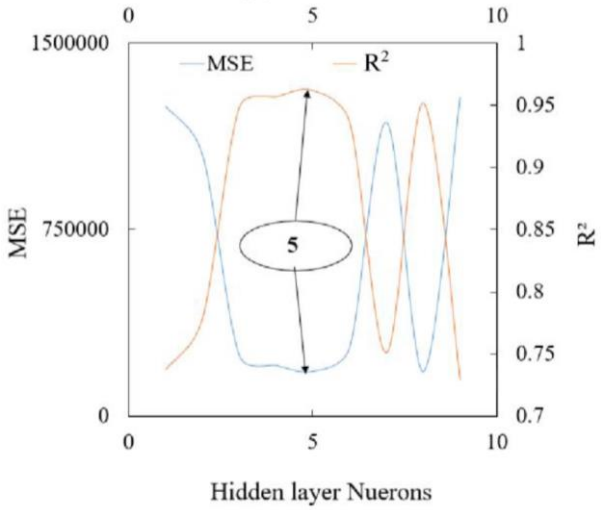

(b) D/W=1

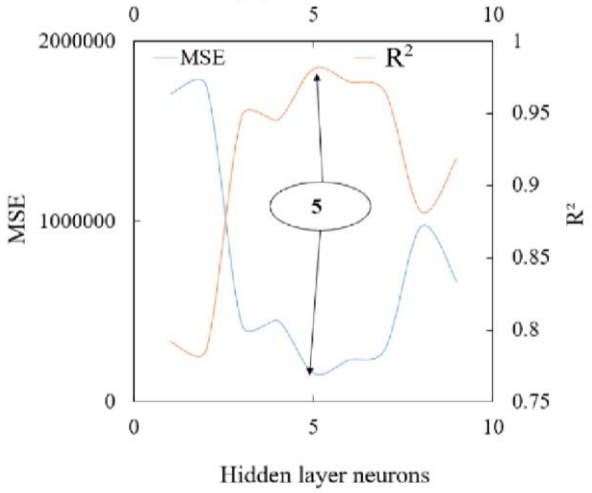

(c) D/W=2

Fig. 3. Estimation of the optimum number of hidden layer neuron at different embedment ratio.

Figure 3 shows how the R^2 and MSE affect the hidden layer neurons. Figure 3 indicates that the R^2 and MSE observed were highest and minimum at 5 hidden layer neurons, respectively, and that as the number of hidden layer neurons rises, either R^2 declines or MSE increases for each of the embedment ratios. A model structure with 7 input variables, 1 hidden layer, 5 hidden layer neurons, and 1 output layer was chosen based on this investigation. Figure 4 displays the completed network.

To verify the generated model's prediction accuracy, the bearing capacity (BC_{DP}) obtained from the model was compared to the actual bearing capacity (BC_{DA}). Equations (2 to 7) describe the model's equations for measuring characteristics such as correlation coefficient (r), coefficient of determination (R^2), mean square error (MSE), root mean square error (RMSE), mean absolute error (MAE), and mean absolute percentage error (MAPE).

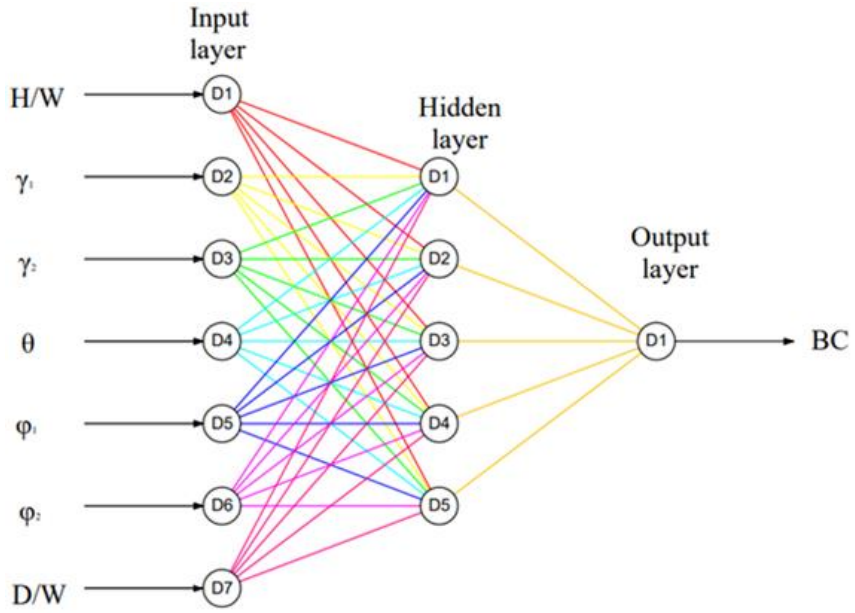

Fig. 4. Architecture of the model.

$$\text{Correlation coefficient } (r) \qquad r = \frac{\sum_{i=1}^{n}\left(BC_{DAi} * BC_{DPi} - \overline{BC_{DAi}} * \overline{BC_{DPi}}\right)}{(n-1)S_{DAi}S_{DPi}} \tag{2}$$

$$\text{Cefficient of determination } (R^2) \qquad R^2 = 1 - \frac{\sum_{i=1}^{n}\left(BC_{DAi} - BC_{DPi}\right)^2}{\sum_{i=1}^{n}\left(BC_{DAi} - \overline{BC_{DAi}}\right)^2} \tag{3}$$

$$\text{Mean square error } (MSE) \qquad MSE = \frac{1}{n}\sum_{i=1}^{n}\left(BC_{DAi} - BC_{DPi}\right)^2 \tag{4}$$

$$\text{Root mean square error } (RMSE) \qquad RMSE = \sqrt{\frac{1}{n}\sum_{i=1}^{n}\left(BC_{DAi} - BC_{DPi}\right)^2} \tag{5}$$

$$\text{Mean absolute error } (MAE) \qquad MAE = \frac{1}{n}\sum_{i=1}^{n}\left|BC_{DAi} - BC_{DPi}\right| \tag{6}$$

$$\textit{Mean absolute percentage error } (MAPE) \qquad MAPE = \left(\frac{1}{n} \sum_{i=1}^{n} \frac{\left| BC_{DAi} - BC_{DPi} \right|}{\left| BC_{DAi} \right|} \right) * 100 \qquad (7)$$

Note: BC_{DAi}, BC_{DPi} : actual and predicted bearing capacity respectively, $\overline{BC_{DAi}}$, $\overline{BC_{DPi}}$: mean of actual and predicted bearing capacity respectively, S_{DAi}, S_{DPi} : Standard deviation of actual and predicted bearing capacity respectively, n: number of observations.

Table 3
Assessing parameters for the developed **model** at different embedment ratio.

D/W	Assessing parameters	Training	Testing
0	r	0.99	0.98
	R^2	0.98	0.97
	MSE	12863.50	32408.40
	RMSE	113.41	180.02
	MAE	81.73	131.60
	MAPE (%)	8.82	0.03
1	r	0.98	0.97
	R^2	0.96	0.95
	MSE	179453.60	349926.50
	RMSE	423.61	591.54
	MAE	269.88	370.14
	MAPE (%)	9.40	0.003
2	r	0.99	0.98
	R^2	0.98	0.97
	MSE	158080.40	333542.56
	RMSE	397.59	577.53
	MAE	283.17	410.98
	MAPE (%)	6.27	0.002

The constructed model's assessment statistical parameters (r, R^2, MSE, RMSE, MAE, and MAPE) were summarized in Table 3 for both the training and testing data. At embedment ratios of 0, 1, and 2, the coefficient of correlation (r) of the constructed model was determined to be 0.99, 0.98, and 0.99 for training data and 0.98, 0.97, and 0.98 for testing data. The relative correlation and goodness-of-fit between the predicted and actual values are represented by the coefficient of correlation. |r| should fall between 0.0 and 1.0. In fact, the correlation must have a r value between zero and one, which is a necessary condition but not a sufficient one condition. In machine learning, the only acceptable correlations are those that are close to one. Table 3 further demonstrates that all the evaluating parameters are within acceptable limits. Figures 5 and 6 show the contrast between the BC_{DP} calculated by the neural network and the real BC_{DA} for the training and testing data, respectively. Figures 5 and 6 shows that for both training and testing data, the predicted and actual values of bearing capacity have coefficients of determination (R^2) greater than 0.95, indicating a good fit for the data and the model developed could be used to predict the output. The final connection weights between the input layers to the hidden layer [x_{Dij}] and the hidden layer to the output layer [y_{Djk}], input bias [z_{Dj}] and output bias [z_D], as well as the matrices of correlation created, are shown as follows.

Generalized form of matrices: -

$$x_{Dij} = \begin{bmatrix} x_{D11} & x_{D12} & x_{D13} & x_{D14} & x_{D15} & x_{D16} & x_{D17} \\ x_{D21} & x_{D22} & x_{D23} & x_{D24} & x_{D25} & x_{D26} & x_{D27} \\ x_{D31} & x_{D32} & x_{D33} & x_{D34} & x_{D35} & x_{D36} & x_{D37} \\ x_{D41} & x_{D42} & x_{D43} & x_{D44} & x_{D45} & x_{D46} & x_{D47} \\ x_{D51} & x_{D52} & x_{D53} & x_{D54} & x_{D55} & x_{D56} & x_{D57} \end{bmatrix}, \quad y_{Djk} = \begin{bmatrix} y_{D11} \\ y_{D21} \\ y_{D31} \\ y_{D41} \\ y_{D51} \end{bmatrix}, \quad z_{Dj} = \begin{bmatrix} z_{D1} \\ z_{D2} \\ z_{D3} \\ z_{D4} \\ z_{D5} \end{bmatrix}, \quad z_D = \begin{bmatrix} z_D \end{bmatrix} \tag{8}$$

Matrices for D/W = 0

$$x_{1ij} = \begin{bmatrix} -3.40 & -0.55 & -0.85 & 3.76 & -0.53 & -0.90 & 1.37 \\ 1.69 & -1.45 & -0.17 & 5.27 & -1.48 & -0.30 & -0.51 \\ 0.78 & -0.12 & -0.26 & 5.12 & -0.14 & -0.34 & -2.92 \\ -3.31 & -1.63 & -1.27 & 9.77 & -1.49 & -1.32 & 4.37 \\ -3.81 & 0.69 & -0.02 & -1.39 & 0.68 & 0.06 & 0.44 \end{bmatrix}, \quad y_{1jk} = \begin{bmatrix} -1.46 \\ -1.81 \\ -3.77 \\ -5.47 \\ -2.59 \end{bmatrix}, \quad z_{1j} = \begin{bmatrix} 1.35 \\ -0.45 \\ -2.91 \\ 4.24 \\ 0.34 \end{bmatrix}, \quad z_1 = \begin{bmatrix} 6.60 \end{bmatrix} \tag{9}$$

Matrices for D/W = 1

$$x_{2ij} = \begin{bmatrix} 2.53 & 0.45 & 0.14 & -1.67 & 0.37 & 0.24 & -1.90 \\ -0.12 & -0.17 & -0.33 & 6.72 & -0.17 & -0.22 & -3.36 \\ -5.33 & -1.88 & -2.20 & 4.53 & -1.88 & -2.27 & 6.41 \\ -10.24 & 0.08 & 0.05 & -0.70 & 0.07 & 0.09 & -0.55 \\ -1.78 & 0.43 & -0.68 & 4.32 & -0.50 & -0.70 & 0.54 \end{bmatrix}, \quad y_{2jk} = \begin{bmatrix} 1.27 \\ -5.94 \\ -4.56 \\ -4.27 \\ -1.74 \end{bmatrix}, \quad z_{2j} = \begin{bmatrix} 1.94 \\ -3.22 \\ -6.35 \\ -0.62 \\ 0.58 \end{bmatrix}, \quad z_2 = \begin{bmatrix} 4.65 \end{bmatrix} \tag{10}$$

Matrices for D/W = 2

$$x_{3ij} = \begin{bmatrix} -0.72 & 1.24 & 0.74 & -0.94 & -0.19 & 0.91 & -1.11 \\ -1.46 & 3.32 & -1.02 & -0.06 & 0.65 & -0.97 & -0.06 \\ -4.46 & -4.89 & -1.00 & -1.33 & 4.20 & -1.02 & -1.19 \\ -5.05 & -1.48 & -0.36 & -0.20 & 0.48 & -0.29 & -0.22 \\ -0.08 & 7.27 & -0.28 & 0.01 & -3.80 & -0.19 & 0.02 \end{bmatrix}, \quad y_{3jk} = \begin{bmatrix} -0.83 \\ -1.69 \\ -4.94 \\ -2.39 \\ -6.07 \end{bmatrix}, \quad z_{3j} = \begin{bmatrix} -0.20 \\ 0.57 \\ 4.16 \\ 0.62 \\ -3.89 \end{bmatrix}, \quad z_3 = \begin{bmatrix} 5.39 \end{bmatrix} \tag{11}$$

Here:

$[x_{Dji}]$ = connection weight of i^{th} hidden layer neuron and i^{th} input layer neuron respectively for each set of data at different embedment ratio

$[y_{Djk}]$ = connection weight of the k^{th} output layer neuron and j^{th} hidden layer neuron respectively for each set of data at different embedment ratio.

$[z_{Dj}]$ = bias for j^{th} hidden layer neuron respectively for each set of data at different embedment ratio

$[z_D]$ = bias for output layer for respectively for each set of data at different embedment ratio

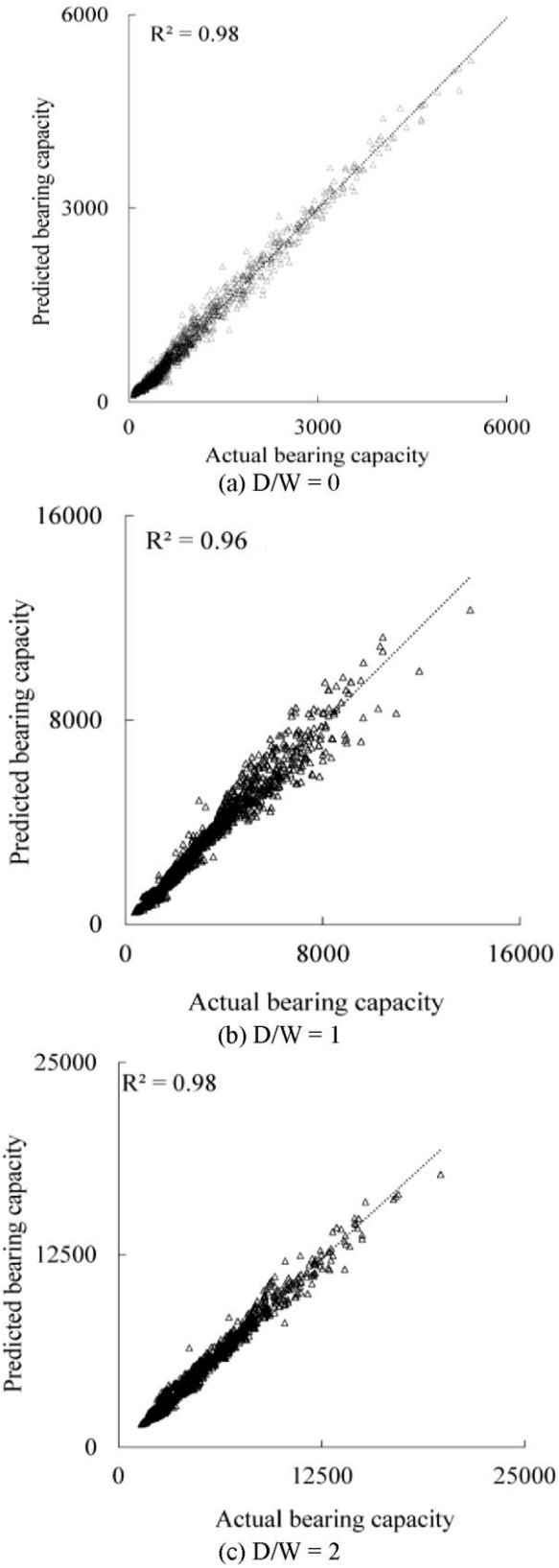

Fig. 5. Comparison of predicted bearing capacity with the actual bearing capacity for the training (a, b and c) data at different embedment ratio.

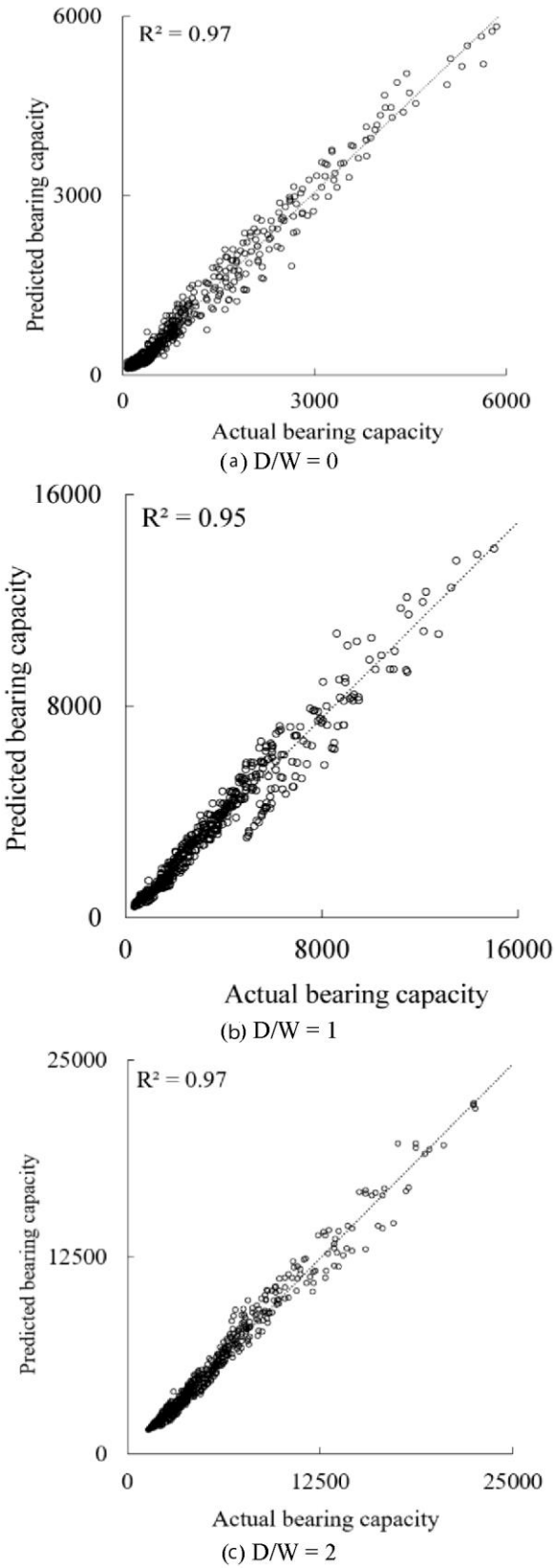

Fig. 6. Comparison of predicted bearing capacity with the actual bearing capacity for the testing (a, b and c) data at different embedment ratio.

5. Sensitivity analysis

By using sensitivity analysis, this section of the study examines the impact of various factors on output bearing capacity. Sensitivity analysis was performed using a method described by [32] and based on the weight configuration. However, because it estimates the value of absolute weights, this method has its own limitations. It was reported by [33] that another approach to circumvent this issue, and this method was used to do the sensitivity analysis. For every input neuron, this method estimates the sum of the finalized connection weight from the input layer neuron to the hidden layer neurons plus connection weights from the hidden layer neurons to the output layer neuron. Equation (12) is used to calculate the contribution of each individual variable to a given input.

$$IR_{Dj} = \sum_{k=1}^{h} x_{Djk} * x_k \tag{12}$$

here:

x_{Djk} = connection weight between k^{th} neuron of the hidden layer and j^{th} input variable.
x_k = connection weight between the single output neuron and the k^{th} neuron of a hidden layer.
IRj = relative importance of the j^{th} neuron in the input layer
h = number of the hidden layer neurons.
The relative influence of the individual input variable on output bearing capacity using equation (12) was shown in Figures 7, 8 and 9.

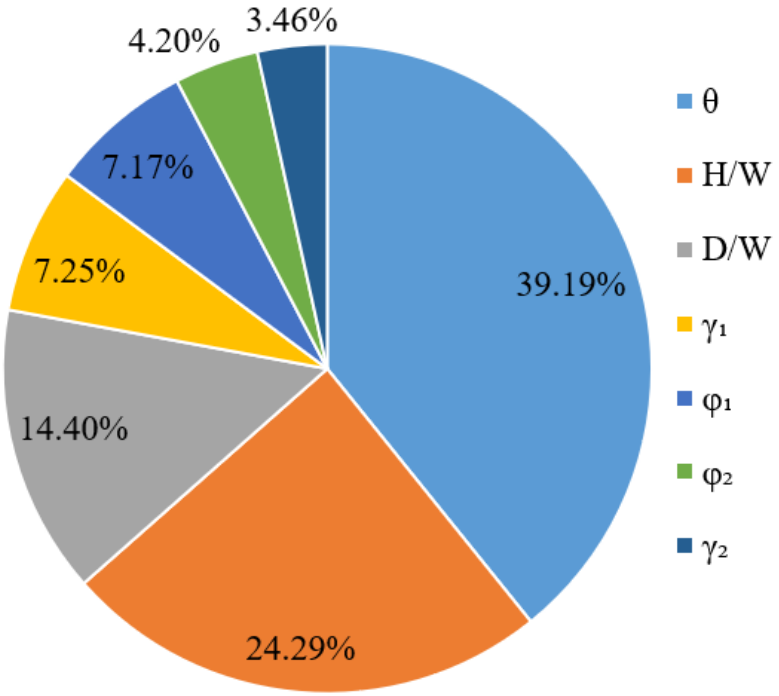

Fig. 7. Sensitivity analysis of the individual variable on the output bearing capacity at an embedment ratio of 0.

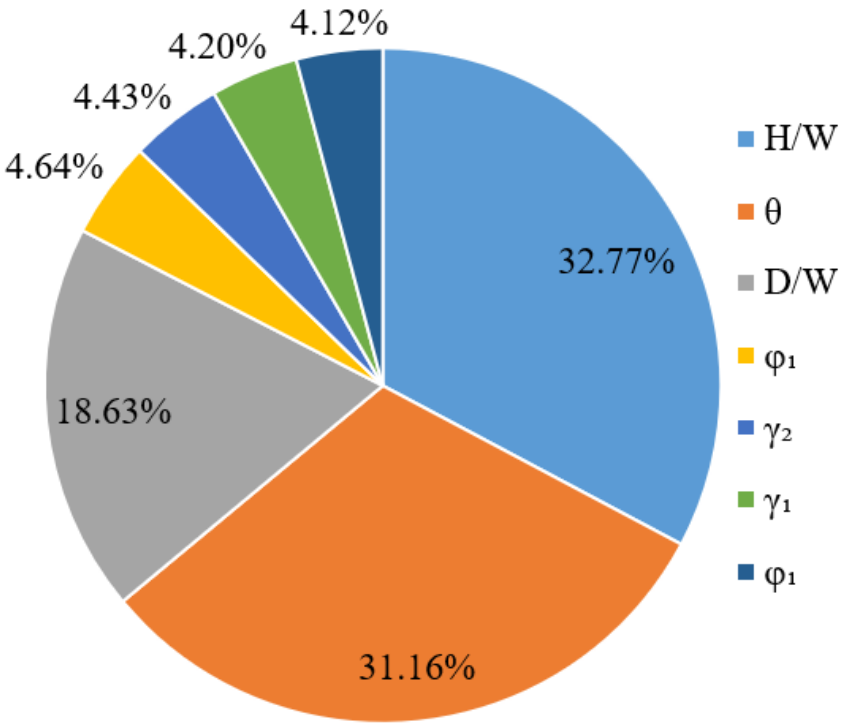

Fig. 8. Sensitivity analysis of the individual variable on the output bearing capacity at an embedment ratio of 1.

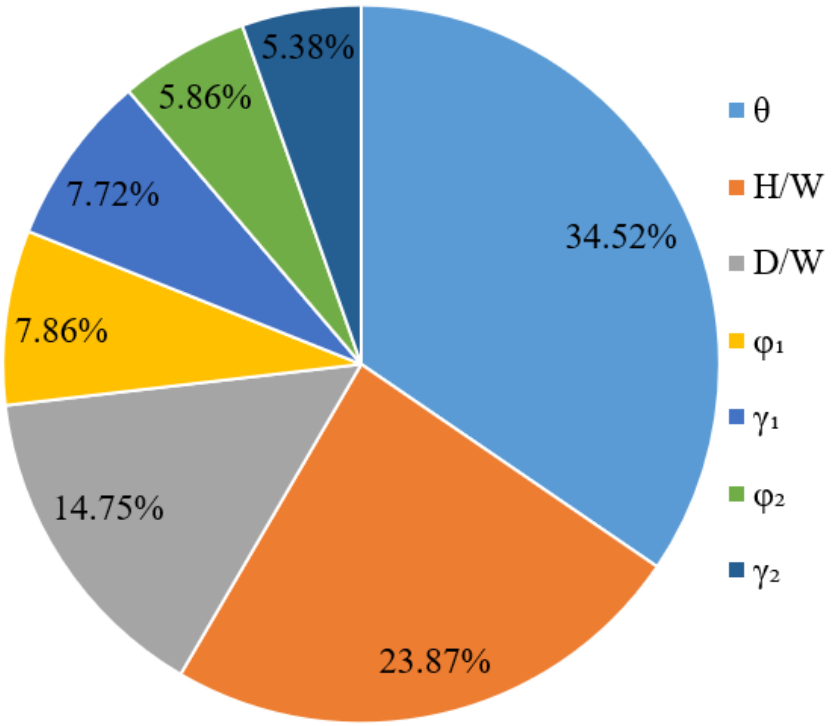

Fig. 9. Sensitivity analysis of the individual variable on the output bearing capacity at an embedment ratio of 2.

Study of Figures 7, 8 and 9 reveals that the output bearing capacity was mostly influenced by the load inclination (θ) at an embedment ratio 0, 1 and 2 i.e. 39.19 %, 32.77 % and 34.52 %

respectively. The difference between the most influencing input (H/W and θ) variables is very small (1.61 %) for an embedment ratio of 1, hence it can be stated that the most influencing input variable is load inclination to output bearing capacity. This could be because when the load inclination rises, the horizontal displacement of the footing rises, causing the rectangular footing to break. As a result, the load inclination has the greatest influence on the output bearing capacity at all embedment ratios. The order for the other input variable to influence the output was as H/W>D/W> γ_1 >φ_1> φ_2 >γ_2, θ> D/W> φ_1> γ_2> γ_1> φ_2 and H/W> D/W> φ_1 >γ_1> φ_2 > γ_2 for embedment ratio 0, 1 and 2 respectively. Again, as the thickness of the upper layer of dense soil increases, so does the bearing capacity, and as the depth of the footing from the top surface of upper dense soil increases, so does the surcharge load and, as a result, the bearing capacity. The output is also influenced by upper dense soil properties, since denser sand has better grain to grain interlocking than loose sand. Thus, it can be concluded that performing sensitivity analysis is an effective way to physically connect the input variables with the output bearing capacity.

6. Proposed model

The weights and biases obtained are used for the development of a model equation as per [34]. The generated optimal weights and biases are presented by equations (8 to 11), the model takes the following form as per equation (13):

$$BC_{DP} = \left[q_u\right]_{\langle H/W,\theta,\varphi_1,\varphi_2,\gamma_1,\gamma_2,D/W\rangle} = fn\left\{z_D + \sum_{i=1}^{h}\left[y_{Djk}\, f_n\left(\sum_{i=1}^{n} x_{Dij} F_{Di}\right)\right]\right\} \tag{13}$$

Here;
h = number of hidden layer neuron

F_{Di} = normalized inputs in the range of 0 to 1.

fn = sigmoid activation function

n = number of input variables

The equations (14 to 16) show the generalized form of expressions to convert the optimal connections weight matrices in the required model equation. The following steps as shown in equations 16(a-e) and 17(a-e) were carried out using the generalized equations for embedment ratio 0. The final expression is shown in the equation (18) and equation (19) for embedment ratio 0.

$$A_{Di} = x_{\mathrm{Di1}} * \left(\frac{H}{W}\right) + x_{\mathrm{Di2}} * \left(\gamma_1\right) + x_{\mathrm{Di3}} * \left(\gamma_2\right) + x_{\mathrm{Di4}} * \left(\theta\right) + x_{\mathrm{Di5}} * \left(\varphi_1\right) + x_{\mathrm{Di5}} * \left(\varphi_2\right) + x_{\mathrm{Di6}} * \left(\frac{D}{W}\right) + z_{Di} \tag{14}$$

$$B_{Dj} = \left(\frac{y_{\mathrm{Djk}}}{1 + e^{(-2*0.5*A_{21})}}\right) \tag{15}$$

$$BC_{DP} = \sum_{i=0}^{n}\left(B_{Dj}\right) + z_D \tag{16}$$

For D/W = 0,

$$A_{11} = x_{111} * \left(\frac{H}{W}\right) + x_{112} * \left(\gamma_1\right) + x_{113} * \left(\gamma_2\right) + x_{114} * \left(\theta\right) + x_{115} * \left(\varphi_1\right) + x_{115} * \left(\varphi_2\right) + x_{116} * \left(\frac{D}{W}\right) + z_{111} \tag{16(a)}$$

$$A_{12} = x_{121} * \left(\frac{H}{W}\right) + x_{122} * \left(\gamma_1\right) + x_{123} * \left(\gamma_2\right) + x_{124} * \left(\theta\right) + x_{125} * \left(\varphi_1\right) + x_{125} * \left(\varphi_2\right) + x_{126} * \left(\frac{D}{W}\right) + z_{12} \tag{16(b)}$$

$$A_{13} = x_{131} * \left(\frac{H}{W}\right) + x_{132} * \left(\gamma_1\right) + x_{133} * \left(\gamma_2\right) + x_{134} * \left(\theta\right) + x_{135} * \left(\varphi_1\right) + x_{135} * \left(\varphi_2\right) + x_{136} * \left(\frac{D}{W}\right) + z_{13} \tag{16(c)}$$

$$A_{14} = x_{141} * \left(\frac{H}{W}\right) + x_{142} * \left(\gamma_1\right) + x_{143} * \left(\gamma_2\right) + x_{144} * \left(\theta\right) + x_{145} * \left(\varphi_1\right) + x_{145} * \left(\varphi_2\right) + x_{146} * \left(\frac{D}{W}\right) + z_{14} \tag{16(d)}$$

$$A_{15} = x_{151} * \left(\frac{H}{W}\right) + x_{152} * \left(\gamma_1\right) + x_{153} * \left(\gamma_2\right) + x_{154} * \left(\theta\right) + x_{155} * \left(\varphi_1\right) + x_{155} * \left(\varphi_2\right) + x_{156} * \left(\frac{D}{W}\right) + z_{15} \tag{16(e)}$$

$$B_{11} = \left(\frac{y_{111}}{1 + e^{(-A_{11})}}\right) \tag{17(a)}$$

$$B_{12} = \left(\frac{y_{121}}{1 + e^{(-A_{12})}}\right) \tag{17(b)}$$

$$B_{13} = \left(\frac{y_{131}}{1 + e^{(-A_{13})}}\right) \tag{17(c)}$$

$$B_{14} = \left(\frac{y_{141}}{1 + e^{(-A_{14})}}\right) \tag{17(d)}$$

$$B_{15} = \left(\frac{y_{151}}{1 + e^{(-A_{15})}}\right) \tag{17(e)}$$

$$C_{1P} = \left[q_u\right]_{\left\langle H/W, \theta, \varphi_1, \varphi_2, \gamma_1, \gamma_2, D/W \right\rangle} = z_1 + B_{11} + B_{12} + B_{13} + B_{14} + B_{15} \tag{18}$$

$$C_1 = 6.60 - \frac{1.46}{1 + \exp^{(-A_{11})}} - \frac{1.81}{1 + \exp^{(-A_{12})}} - \frac{3.77}{1 + \exp^{(-A_{13})}} - \frac{5.47}{1 + \exp^{(-A_{14})}} - \frac{2.59}{1 + \exp^{(-A_{15})}} \tag{19}$$

$$BC_{1P} = \frac{1}{1 + \exp^{(-C_1)}} \tag{20}$$

Similar steps (from 16(a-e),17(a-e) and 19) are followed for embedment ratio 1 and 2 and the finally obtained expression are shown in the equation (22) and equation (24).

For D/W = 1,

$$C_2 = 4.65 + \frac{1.27}{1+\exp^{(-A_{21})}} - \frac{5.94}{1+\exp^{(-A_{22})}} - \frac{4.56}{1+\exp^{(-A_{23})}} - \frac{4.27}{1+\exp^{(-A_{24})}} - \frac{1.74}{1+\exp^{(-A_{25})}} \tag{21}$$

$$BC_{2P} = \frac{1}{1+\exp^{(-C_2)}} \tag{22}$$

For D/W = 2,

$$C_3 = 5.39 - \frac{0.83}{1+\exp^{(-A_{31})}} - \frac{1.69}{1+\exp^{(-A_{32})}} - \frac{4.94}{1+\exp^{(-A_{33})}} - \frac{2.36}{1+\exp^{(-A_{34})}} - \frac{6.07}{1+\exp^{(-A_{35})}} \tag{23}$$

$$BC_{3P} = \frac{1}{1+\exp^{(-C_3)}} \tag{24}$$

The bearing capacity equations (20, 22 and 24) can be presented in the denormalized form using a generalized expression as per equation (25) and are shown in equation (26), equation (27) and equation (28) at embedment ratio 0, 1 and 2 respectively.

$$\left[q_u\right]_{\langle H/W,\theta,\varphi_1,\varphi_2,\gamma_1,\gamma_2,D/W\rangle} = BC_{DP} = 0.5\left(BC_{DP}+1\right)\left[\left(BC_{DP}\right)_{\max} - \left(BC_{DP}\right)_{\min}\right] + \left(BC_{DP}\right)_{\min} \tag{25}$$

$$\left[q_u\right]_{\langle H/W,\theta,\varphi_1,\varphi_2,\gamma_1,\gamma_2,0\rangle} = BC_{1P} = 0.5\left(BC_{1P}+1\right)\left[6137.50\right] + 75.41 \tag{26}$$

$$\left[q_u\right]_{\langle H/W,\theta,\varphi_1,\varphi_2,\gamma_1,\gamma_2,1\rangle} = BC_{2P} = 0.5\left(BC_{2P}+1\right)\left[13601.69\right] + 371.62 \tag{27}$$

$$\left[q_u\right]_{\langle H/W,\theta,\varphi_1,\varphi_2,\gamma_1,\gamma_2,2\rangle} = BC_{3P} = 0.5\left(BC_{3P}+1\right)\left[18427.80\right] + 1398.63 \tag{28}$$

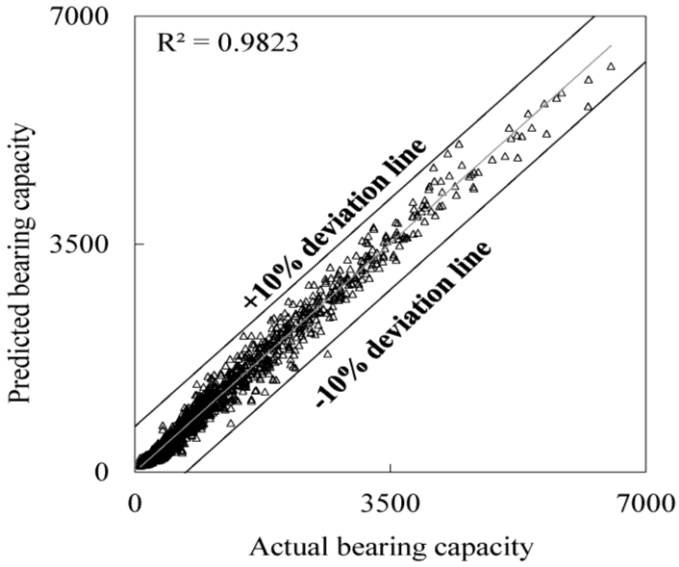

Fig. 10. Comparison between the actual bearing capacity and the predicted bearing capacity using model equations at an embedment ratio of 0.

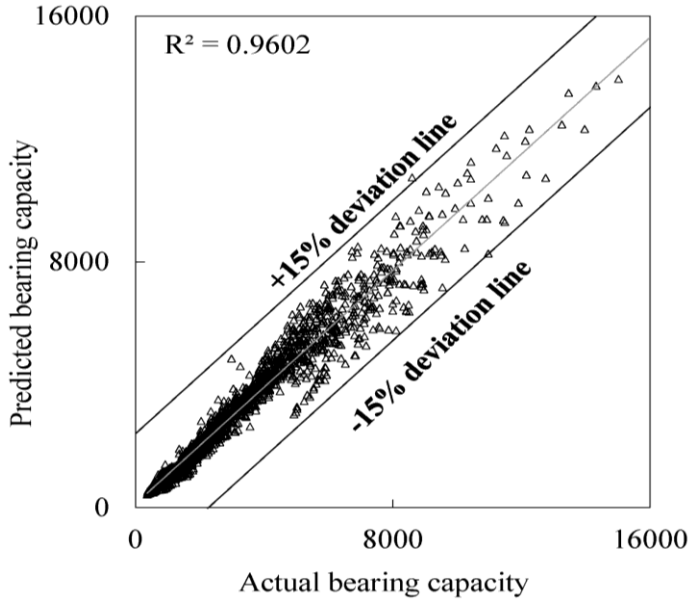

Fig. 11. Comparison between the actual bearing capacity and the predicted bearing capacity using model equations at an embedment ratio of 0.

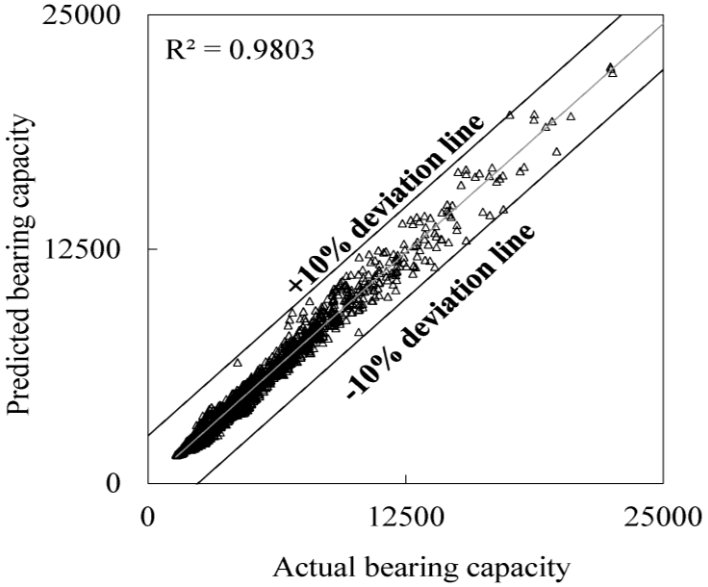

Fig. 12. Comparison between the actual bearing capacity and the predicted bearing capacity using model equations at an embedment ratio of 2.

Based on the data collected as per [5,13], the final model expressions are proposed through equation (26), equation (27) and equation (28) at embedment ratio 0, 1 and 2 respectively. These equations can be used to predict the ultimate bearing capacity of the rectangular footing on the layered sand under the influence of inclined loading. Figures 10, 11 and 12 shows the comparison between the actual bearing capacity and the predicted bearing capacity determined by using model equation (26), equation (27) and equation (28). Study of Figures 10, 11 and 12 reveals that the deviation between the predicted bearing capacity and the actual bearing capacity was ±10%, ±15% and ±10% at an embedment ratio 0, 1 and 2 respectively. Normally acceptable

range of error is supposed to be within ±10% for predictions in the field of geotechnical engineering as per [35]. Therefore, the proposed models can be effectively used for the prediction of the bearing capacity of the rectangular footing resting on layered soil under inclined loading.

6.1. Comparison

Using an approach based on machine learning, the experimental results reported in [36] were compared to the results predicted by the current study. The dimensionless bearing capacity obtained from this study for L/W=1.5 was calculated and compared to the results reported by [36] for the circular footing. It is important to note that [36] determined the friction angle and unit weight of the upper dense and lower loose sand layers to be 47.5° and 34°, respectively, and 16.33 kN/m^3 and 13.78 kN/m^3. 50 mm was the diameter of the circular footing and 600 mm x 200 mm x 500 mm was the size of the model used in the experimental work. The comparison was depicted in Table 4 for a load inclination of 0°, 10°, 20°, and 30° at a thickness ratio of 1. Table 4 reveals that the bearing capacity of the circular footing decreased by 79.00 % when the load inclination was increased from 0° to 30°, as shown by the results of [36] presented in Table 4. The associated comparison shown in Table 4 suggests that the current results compare favourably with a standard deviation of 21.99% in the dimensionless bearing capacity. The difference between the current results and those of [36] can be attributed to the difference in the shape factors of the footing considered for comparison.

Table 4
Comparison of present results for L/W=1.5 at H/W =1 and φ_1= 46° & φ_2= 34° with literature.

Load inclination	Dimensionless bearing capacity ($q_u/\gamma_1 W$)	
	Meyerhof and Hanna [36]	Present study
	φ_1= 47.5° & φ_2= 34°	φ_1= 46° & φ_2= 34°
0°	58.26	81.12
10°	40.49	52.43
20°	26.30	36.07
30°	12.23	21.37

7.Conclusions

Using a machine learning approach, the current research aims to build model equations for the bearing capacity of a rectangular foundation built on layered sand under the effect of inclined loading. The independent variables utilised to predict the output bearing capacity were thickness ratio (H/W), load inclination angle (θ), unit weight of higher dense (γ_1) and lower loose sand layer (γ_2), Friction angle of upper dense (φ_1) and lower loose sand (φ_2) layer and embedment ratio (D/W) with BC_{DP} as an output. Following conclusions can be drawn based on the discussions as given below: -

1. The sigmoid activation function obtained to predict output bearing capacity of the rectangular footing on layered sand under inclined loading are same corresponding to an embedment ratio of 0, 1 and 2.

2. All the assessing parameter (r, R^2, MSE, RMSE, MAE, MAPE) are observed to be optimum for the sigmoid activation function.
3. The coefficient of determination for training and testing data observed to be 0.98 and 0.97, 0.96 and 0.95, 0.98 and 0.97 at embedment ratio 0, 1 and 2 respectively.
4. The mean absolute percentage error for training and testing data lies at 8.82, 9.40, 6.27 and 0.03, 0.003, 0.002 corresponding to an embedment ratio 0, 1 and 2 respectively.
5. The most influencing input variable to affect the output bearing capacity at embedment ratio 0, 1 and 2 was load inclination and its relative importance was 39.19 %, 32.77 % and 34.52 % respectively.
6. The deviation between the actual bearing capacity and predicted bearing capacity was ±10%, ±15% and ±10% at an embedment ratio 0, 1 and 2 respectively.

The primary purpose of this research was to establish how to use machine learning to forecast the bearing capacity of a rectangular foundation on layered sand under the influence of inclined loading. The presented models can predict the bearing capacity at different embedment ratios within the variance allowed. Using numerical or machine learning techniques, the rectangular footing on layered sand subjected to eccentric inclined loading must be explored further. In addition, the proposed formulas in this work will assist researchers in eliminating the need to conduct time- and cost-intensive experimental or numerical studies.

Funding

This research did not receive any outside funding.

Conflicts of interest

There are no conflicts of interest declared by the authors.

Authors contribution statement

VP: Conceptualization; RKD: Data curation; VP: Formal analysis; VP: Investigation; RKD: Methodology; RKD: Project administration; VP: Resources; VP: Software; RKD: Supervision; VP: Validation; VP: Visualization; VP: Roles/Writing – original draft; RKD, VP: Writing – review & editing.

References

[1] Kumar J, Chakraborty M. Bearing capacity of a circular foundation on layered sand–clay media. Soils Found 2015;55:1058–68. https://doi.org/10.1016/j.sandf.2015.09.008.

[2] Joshi VC, Dutta RK, Shrivastava R. Ultimate bearing capacity of circular footing on layered soil. J Geoengin 2015;10:25–34.

[3] Khatri VN, Kumar J, Akhtar S. Bearing Capacity of Foundations with Inclusion of Dense Sand Layer over Loose Sand Strata. Int J Geomech 2017;17. https://doi.org/10.1061/(ASCE)GM.1943-5622.0000980.

[4] Mosadegh A, Nikraz H. Bearing capacity evaluation of footing on a layered-soil using ABAQUS. J Earth Sci Clim Change 2015;6:1000264.

[5] Panwar V, Dutta RK. Numerical study of ultimate bearing capacity of rectangular footing on layered sand. J Achiev Mater Manuf Eng 2020;1:15–26. https://doi.org/10.5604/01.3001.0014.4087.

[6] Rao P, Liu Y, Cui J. Bearing capacity of strip footings on two-layered clay under combined loading. Comput Geotech 2015;69:210–8. https://doi.org/10.1016/j.compgeo.2015.05.018.

[7] Mosallanezhad M, Moayedi H. Comparison Analysis of Bearing Capacity Approaches for the Strip Footing on Layered Soils. Arab J Sci Eng 2017;42:3711–22. https://doi.org/10.1007/s13369-017-2490-6.

[8] Khatri VN, Singh N, Dutta RK, Yadav JS. Numerical Estimation of Bearing Capacity of Shallow Footings Resting on Layered Sand. Transp Infrastruct Geotechnol 2022. https://doi.org/10.1007/s40515-022-00236-4.

[9] Das PP, Khatri VN, Doley R, Dutta RK, Yadav JS. Estimation of bearing capacity of shallow footings on layered sand using finite elements analysis. J Eng Des Technol 2022. https://doi.org/10.1108/JEDT-09-2021-0493.

[10] Zheng G, Zhao J, Zhou H, Zhang T. Ultimate bearing capacity of strip footings on sand overlying clay under inclined loading. Comput Geotech 2019;106:266–73. https://doi.org/10.1016/j.compgeo.2018.11.003.

[11] Dutta RK, Khatri VN, Kaundal N. Ultimate Bearing Capacity of Strip Footing on Sand Underlain By Clay Under Inclined Load. Civ Environ Eng Reports 2022;32:116–37. https://doi.org/10.2478/ceer-2022-0007.

[12] Singh SP, Roy AK. Numerical Study of the Behaviour of a Circular Footing on a Layered Granular Soil Under Vertical and Inclined Loading. Civ Environ Eng Reports 2021;31:29–43. https://doi.org/10.2478/ceer-2021-0002.

[13] Panwar V, Dutta RK. Bearing capacity of rectangular footing on layered sand under inclined loading. J Achiev Mater Manuf Eng 2021;108:49–62. https://doi.org/10.5604/01.3001.0015.5064.

[14] Nazeer S, Dutta RK. Application of Machine Learning Techniques in Predicting the Bearing Capacity of E-shaped Footing on Layered Sand. J Soft Comput Civ Eng 2021;5:74–89. https://doi.org/10.22115/scce.2021.303113.1360.

[15] Dutta RK, Gnananandarao T, Sharma A. Application of random forest regression in the Prediction of ultimate bearing capacity of strip footing resting on dense sand overlying loose sand deposit. J Soft Comput Civ Eng 2019;3:28–40.

[16] Sasmal SK, Behera RN. Prediction of combined static and cyclic load-induced settlement of shallow strip footing on granular soil using artificial neural network. Int J Geotech Eng 2021;15:834–44. https://doi.org/10.1080/19386362.2018.1557384.

[17] Gor M. Analyzing the bearing capacity of shallow foundations on two-layered soil using two novel cosmology-based optimization techniques. Smart Struct Syst 2022;29:513–22.

[18] Moayedi H, Gör M, Kok Foong L, Bahiraei M. Imperialist competitive algorithm hybridized with multilayer perceptron to predict the load-settlement of square footing on layered soils. Measurement 2021;172:108837. https://doi.org/10.1016/j.measurement.2020.108837.

[19] Moayedi H, Gör M, Khari M, Foong LK, Bahiraei M, Bui DT. Hybridizing four wise neural-metaheuristic paradigms in predicting soil shear strength. Measurement 2020;156:107576. https://doi.org/10.1016/j.measurement.2020.107576.

[20] Bui, Moayedi, Gör, Jaafari, Foong. Predicting Slope Stability Failure through Machine Learning Paradigms. ISPRS Int J Geo-Information 2019;8:395. https://doi.org/10.3390/ijgi8090395.

[21] Dutta RK, Gnananandarao T, Khatri VN. Application of Soft Computing Techniques in Predicting the Ultimate Bearing Capacity of Strip Footing Subjected to Eccentric Inclined Load and Resting on Sand. J Soft Comput Civ Eng 2019;3:30–42.

[22] Ebid AM, Onyelowe KC, Salah M. Estimation of Bearing Capacity of Strip Footing Rested on Bilayered Soil Profile Using FEM-AI-Coupled Techniques. Adv Civ Eng 2022;2022:1–11. https://doi.org/10.1155/2022/8047559.

[23] Moayedi H, Abdullahi MM, Nguyen H, Rashid ASA. Comparison of dragonfly algorithm and Harris hawks optimization evolutionary data mining techniques for the assessment of bearing capacity of footings over two-layer foundation soils. Eng Comput 2021;37:437–47. https://doi.org/10.1007/s00366-019-00834-w.

[24] Nazir R, Momeni E, Marsono K, Maizir H. An Artificial Neural Network Approach for Prediction of Bearing Capacity of Spread Foundations in Sand. J Teknol 2015;72. https://doi.org/10.11113/jt.v72.4004.

[25] Kabir MU, Sakib SS, Rahman I, Shahin HM. Performance of ANN Model in Predicting the Bearing Capacity of Shallow Foundations, 2019, p. 695–703. https://doi.org/10.1007/978-981-13-6713-7_55.

[26] Sethy BP, Patra CR, Sivakugan N, Das BM. Prediction of Ultimate Bearing Capacity of Eccentrically Loaded Rectangular Foundations Using ANN, 2018, p. 148–59. https://doi.org/10.1007/978-3-319-63570-5_13.

[27] Sethy BP, Patra C, Das BM, Sobhan K. Prediction of ultimate bearing capacity of circular foundation on sand layer of limited thickness using artificial neural network. Int J Geotech Eng 2021;15:1252–67. https://doi.org/10.1080/19386362.2019.1645437.

[28] Moayedi H, Moatamediyan A, Nguyen H, Bui X-N, Bui DT, Rashid ASA. Prediction of ultimate bearing capacity through various novel evolutionary and neural network models. Eng Comput 2020;36:671–87. https://doi.org/10.1007/s00366-019-00723-2.

[29] Sihag P, Esmaeilbeiki F, Singh B, Ebtehaj I, Bonakdari H. Modeling unsaturated hydraulic conductivity by hybrid soft computing techniques. Soft Comput 2019;23:12897–910. https://doi.org/10.1007/s00500-019-03847-1.

[30] Sihag P, Kumar M, Singh B. Assessment of infiltration models developed using soft computing techniques. Geol Ecol Landscapes 2021;5:241–51. https://doi.org/10.1080/24749508.2020.1720475.

[31] Boger Z, Guterman H. Knowledge extraction from artificial neural network models. 1997 IEEE Int. Conf. Syst. Man, Cybern. Comput. Cybern. Simul., vol. 4, IEEE; n.d., p. 3030–5. https://doi.org/10.1109/ICSMC.1997.633051.

[32] Garson DG. Interpreting neural network connection weights 1991.

[33] Olden JD, Jackson DA. Illuminating the “black box”: a randomization approach for understanding variable contributions in artificial neural networks. Ecol Modell 2002;154:135–50. https://doi.org/10.1016/S0304-3800(02)00064-9.

[34] Goh ATC, Kulhawy FH, Chua CG. Bayesian Neural Network Analysis of Undrained Side Resistance of Drilled Shafts. J Geotech Geoenvironmental Eng 2005;131:84–93. https://doi.org/10.1061/(ASCE)1090-0241(2005)131:1(84).

[35] Bardhan A, Samui P, Ghosh K, Gandomi AH, Bhattacharyya S. ELM-based adaptive neuro swarm intelligence techniques for predicting the California bearing ratio of soils in soaked conditions. Appl Soft Comput 2021;110:107595. https://doi.org/10.1016/j.asoc.2021.107595.

[36] Meyerhof GG, Hanna AM. Ultimate bearing capacity of foundations on layered soils under inclined load. Can Geotech J 1978;15:565–72. https://doi.org/10.1139/t78-060.